THE JOURNAL OF BIOLOGICAL CHEMISTRY VOL. 282, NO. 10, pp. 7232–7241, March 9, 2007
Printed in the U.S.A.

Identification of a Novel Domain at the N Terminus of Caveolin-1 That Controls Rear Polarization of the Protein and Caveolae Formation*

Received for publication, August 3, 2006, and in revised form, December 18, 2006 Published, JBC Papers in Press, January 8, 2007, DOI 10.1074/jbc.M607396200

Xing-Hui Sun[‡], Daniel C. Flynn[§¶], Vincent Castranova[‡‖], Lyndell L. Millecchia[‖], Andrew R. Beardsley[‡], and Jun Liu[‡¶1]

From the Departments of [‡]Physiology and Pharmacology and [§]Microbiology, Immunology, and Cell Biology and the [¶]Mary Babb Randolph Cancer Center, West Virginia University, Morgantown, West Virginia 26506 and the [‖]Pathology and Physiology Research Branch, National Institute for Occupational Safety and Health, Morgantown, West Virginia 26505

When cells are migrating, caveolin-1, the principal protein component of caveolae, is excluded from the leading edge and polarized at the cell rear. The dynamic feature depends on a specific sequence motif that directs intracellular trafficking of the protein. Deletion mutation analysis revealed a putative polarization domain at the N terminus of caveolin-1, between amino acids 32–60. Alanine substitution identified a minimal sequence of 10 residues (^{46}TKEIDLVNRD^{55}) necessary for caveolin-1 rear polarization. Interestingly, deletion of amino acids 1–60 did not prevent the polarization of caveolin-1 in human umbilical vein endothelial cells or wild-type mouse embryonic fibroblasts because of an interaction of Cav_{61-178} mutant with endogenous caveolin-1. Surprisingly, expression of the depolarization mutant in caveolin-1 null cells dramatically impeded caveolae formation. Furthermore, knockdown of caveolae formation by methyl-β-cyclodextrin failed to prevent wild-type caveolin-1 rear polarization. Importantly, genetic depletion of caveolin-1 led to disoriented migration, which can be rescued by full-length caveolin-1 but not the depolarization mutant, indicating a role of caveolin-1 polarity in chemotaxis. Thus, we have identified a sequence motif that is essential for caveolin-1 rear polarization and caveolae formation.

Caveolae are specific microdomains of the plasma membrane that were discovered more than 50 years ago (1). In endothelial cells, numerous vesicles appeared to derive from the uniformly flask-shaped invaginations, suggesting the endocytic potential of caveolae (2). Although the function of caveolae as transport vesicles mediating endocytosis and transcytosis remained obscure (3, 4), the identification, cloning, and characterization of caveolar coat proteins, caveolins, has increased our knowledge of caveolae, and a good body of evidence implicates caveolae in a specialized form of delivery of membrane components, extracellular ligands, bacterial toxins, and nonenveloped virus in several cell types (5–8). The caveolae-mediated endocytic pathway differs from that mediated by clathrin-coated pits. It is sensitive to protein kinase C inhibitors and cholesterol depletion (by filipin), and in some cells it is involved in the activation of protein tyrosine kinases (9). Phosphorylation at tyrosine 14 of caveolin-1 (Cav-1)[2] may be required for the internalization of caveolae. The mechanism controlling caveolae trafficking remains unclear, but it apparently involves both microtubule and actin cytoskeletons (10). Surprisingly, using Cav-1 as a marker for caveolae, recent studies demonstrate that caveolae are rich in a variety of signaling molecules, with the implication that caveolae may function in the regulation of signal transduction. Given these views, an attractive hypothesis would be whether caveolae could carry signaling machinery to different locations of the cell to spatially organize signaling events. Indeed, Anderson and colleagues (11) have shown recently that concomitant with the relocation of caveolae, sites of Ca^{2+} wave initiation moved to the same location in migrating cells.

Three mammalian caveolins, *i.e.* Cav-1, -2, and -3, have been identified and characterized (12). Whereas Cav-1 and -2 are co-expressed in many cell types, Cav-3 is limited to muscle (13–15). Cloning and sequencing of Cav-1 cDNA showed that unlike clathrin, Cav-1 most likely is an integral membrane protein inserted into the membrane so that both the N and C termini of the protein are in the cytosol (16, 17). Biochemical studies have shown that caveolins interact with a variety of signaling molecules, and many of these caveolin-interacting proteins bear a common caveolin binding motif that is recognized by a 20-aa sequence (aa 82–101) proximal to the membrane insertion region. The simultaneous identification of Cav-1 as a caveolar membrane coat and as a component of detergent resistant trans-Golgi-derived vesicle (named VIP21, which stands for vesicular integral membrane protein of 21 kDa) implies that surface caveolin recycles between caveolae and the Golgi apparatus (18). Furthermore, caveolins are implicated in polarized vesicular traffic in epithelia (19) and in cholesterol

* This work was supported by Grant RR016440 from the National Institutes of Health (to J. L. and D. C. F.) and the Sara and James Allen Lung Cancer Funds (to J. L.). The costs of publication of this article were defrayed in part by the payment of page charges. This article must therefore be hereby marked "*advertisement*" in accordance with 18 U.S.C. Section 1734 solely to indicate this fact.

[1] To whom correspondence should be addressed: West Virginia University Health Science Center, Dept. of Physiology and Pharmacology, P. O. Box 9229, Morgantown, WV 26506-9229. Tel.: 304-293-1503; Fax: 304-293-3850; E-mail: junliu@hsc.wvu.edu.

[2] The abbreviations used are: Cav-1, caveolin-1; aa, amino acid(s); ER, endoplasmic reticulum; HUVECs, human umbilical vein endothelial cells; MEFs, mouse embryonic fibroblasts; GFP, green fluorescent protein; N-CPD, N-terminal caveolin polarity domain; FBS, fetal bovine serum; MβCD, methyl-β-cyclodextrin; MES, 4-morpholineethanesulfonic acid; GAPDH, glyceraldehyde-3-phosphate dehydrogenase; Ad, adenovirus.

transport (20, 21). The intracellular trafficking apparently depends on a specific amino acid sequence in caveolin (22, 23).

We and others have shown recently that caveolae and Cav-1 are polarized in migrating endothelial cells (11, 24, 25). However, the mechanism underlying the asymmetrical distribution is not known. It is proposed that polarized caveolae and Cav-1 may play an important role in spatial organization of polarized signaling activity during cell migration, given the fact that caveolae are rich in signaling molecules and actively travel in cells upon stimulation. Indeed, depolarization of Cav-1 by targeted knockdown of the protein significantly impedes cell polarization and inhibits cell directional movement (24). In an attempt to identify specific sequence(s) or domain(s) that controls Cav-1 rear polarization in migrating cells, we generated mutant forms of Cav-1 fused to the reporter protein GFP and expressed them in cells lacking endogenous Cav-1. Here, we report the identification of a novel domain at the N terminus of Cav-1 that controls rear polarization of the protein as well as caveolae formation.

EXPERIMENTAL PROCEDURES

Antibodies and Reagents—pEGFP-N1 and monoclonal antibody for Cav-1 were purchased from BD Biosciences. Protein A/G plus-agarose immunoprecipitation reagent, polyclonal antibodies for GFP and Cav-1 (N-20) were purchased from Santa Cruz Biotechnology (Santa Cruz, CA). Monoclonal anti-FLAG M2 antibody was purchased from Sigma. Rhodamine Red-X-conjugated secondary antibody was obtained from Jackson ImmunoResearch Laboratories (West Grove, PA). BJ5183-AD-1 electroporation-competent cells and pAdTrack-CMV vector were generous gifts from Dr. Bert Vogelstein of The Johns Hopkins Medical Institutions. Cell culture reagents, Lipofectamine™ 2000, and Lipofectin reagent were purchased from Invitrogen. The bicinchoninic acid protein assay kit was purchased from Pierce.

Cell Culture—Primary mouse embryonic fibroblasts (MEFs) were obtained from day 13.5 mouse embryos. Pregnant mice were sacrificed with CO_2 asphyxiation. Embryos were decapitated, thoroughly minced, and trypsinized with 1 ml of 0.05% trypsin in 0.53 mM EDTA (Invitrogen) for 20 min at 37 °C. Ten ml of complete medium (Dulbecco's modified Eagle's medium) supplemented with 10% fetal bovine serum (FBS), 2 mM glutamine, 100 units/ml penicillin, and 100 μg/ml streptomycin (Invitrogen) was used to inactivate the trypsin and resuspend the dissociated cells. Fibroblasts were plated on a 10-cm plate and cultured in a 37 °C, 5% CO_2 incubator. Early passages (passage <5) of primary MEFs were used for all experiments.

Human umbilical vein endothelial cells (HUVECs) were isolated from the human umbilical vein and cultured as described previously (24, 26). The cells were grown in MCDB131 supplemented with 5% heat-inactivated human serum, 20% heat-inactivated newborn calf serum, 150 μg/ml endothelial cell growth supplement, 5 units/ml heparin sodium, 100 units/ml penicillin, and 100 μg/ml streptomycin.

Plasmid Construction and Mutagenesis—The full-length cDNA encoding Cav-1 or mutants was fused in-frame to the N terminus of GFP. EcoRI and BamHI restriction sites were added to the 5′ and 3′ ends of murine Cav-1 cDNA by PCR using the TripleMaster® PCR system (Brinkmann Instruments, Inc.). A series of mutations in Cav-1 were generated by PCR from the cDNA of murine Cav-1 (see Fig. 1). The PCR products were subcloned into the EcoRI and BamHI sites of the pEGFP-N1 eukaryotic expression vector (Clontech). The orientation and sequence of Cav-1-GFP were verified by sequencing.

Cholesterol Depletion—Cholesterol depletion was performed as described previously (27). Briefly, wild-type MEFs were incubated with 0, 3, or 10 mM methyl-β-cyclodextrin (MβCD) in Dulbecco's modified Eagle's medium supplemented with 10% lipid-free FBS for 30 min at 37 °C. Then, the cells were replated onto 1 μg/ml fibronectin-precoated coverglass to allow migration. After a 2-h incubation at 37 °C, cells were fixed for immunofluorescence co-staining with specific antibody for Cav-1 and paxillin or for transmission electron microscopy analysis. The percentage of Cav-1 polarization was calculated.

Adenovirus Production, Amplification, and Purification—FLAG-tagged normal and mutant cDNA of Cav-1 were cloned into pAdTrack-CMV, and the resultant constructs were digested with PmeI and electrotransformed into BJ5183-AD-1-competent cells for recombination. The recombinant adenoviral constructs were purified, digested with PacI, and transfected into AD293 cells to produce the recombinant adenovirus. After 7–10 days, the primary adenovirus was generated. The recombinant adenoviruses were named $AdCav_{1-178}$, $AdCav_{61-178}$, and $AdCav_{46-50A}$. $AdCav_{1-178}$ expressed FLAG-tagged full-length Cav-1 (Cav_{1-178}-FLAG), and $AdCav_{61-178}$ expressed FLAG-tagged N-terminal deletion of Cav-1 (Cav_{61-178}-FLAG). $AdCav_{46-50A}$ expressed Cav-1 with alanine substitution of aa 46–50.

Upon reaching 90% confluency, AD293 cells were infected with the primary adenovirus. The cells were then incubated at 37 °C for 48 h. Following incubation, the cells were collected and suspended in 10 mM Tris-HCl (pH 7.9) buffer. Three freeze/thaw cycles were performed at −20 °C (until completely frozen)/37 °C (until fully thawed). The debris was pelleted, and supernatant was collected for purification. The adenovirus was purified by sequential cesium chloride gradient centrifugation. After purification, the virus was desalted and stored at −80 °C.

Chemotaxis Dunn Chamber Assay—Cav-1 null MEFs infected with $AdCav_{1-178}$, $AdCav_{61-178}$, or AdGFP were seeded on a glass coverslip coated with 0.2% gelatin and starved for 4 h prior to the assay. To set up gradient experiments, both concentric wells of the chamber were filled with starvation medium (Dulbecco's modified Eagle's medium with 0.25% FBS), and a coverslip seeded with cells was inverted onto the chamber in an offset position leaving a narrow slit at one edge for refilling the outer well. The medium of the outer well was drained and replaced with Dulbecco's modified Eagle's medium supplemented with 10% FBS. For control experiments in which cells were subjected to uniform concentrations of chemoattractant, both wells were filled with medium containing 0.25% FBS.

The Horizon Method of Analyzing Chemotaxis—Cells migrating over the annular bridge of the Dunn chamber were recorded using a Zeiss LSM 510 laser-scanning confocal system with 10× objective. Differential interference contrast images were captured at 2-min intervals for a total of 6 h using Zeiss time-lapse software. Only cells migrating at least 20 μm were

included in the calculation. The "horizon" distance was defined as the distance migrated from the starting position by 90% of the cells, a value determined arbitrarily to enable a highly stringent statistical test. Cell trajectories from three independent experiments were tracked manually and converted to a set of angular directions (28). These angles were displayed in a circular histogram where the length of each 18° segment represented the total number of cells with an average angle of migration falling within that particular interval. The Rayleigh test for unimodal clustering of directions was used to determine whether there was a significant chemotactic response (28). A uniform distribution (random cell motility) of data was assumed if the p value for the calculation was greater than 0.05. The mean direction is displayed as an *arrow* and the 95% confidence interval as a *gray arc* (Fig. 8*A*).

Immunofluorescence Microscopy—Cells expressing GFP-tagged normal or mutant forms of Cav-1 were plated on 0.2% gelatin-coated glass coverslips to allow migration, fixed with 2% paraformaldehyde in phosphate-buffered saline for 20 min at 22 °C, and then either mounted with Fluoromount-G (Southern Biotech Inc.) directly or permeabilized with 0.5% (v/v) Triton X-100 for 10 min at 22 °C. The permeabilized cells were blocked with 5% normal goat serum in phosphate-buffered saline for 1 h at 22 °C and incubated with primary antibody for 1 h followed by rhodamine Red-X-conjugated secondary antibody. Fluorescence images of the cells were acquired on an upright Carl Zeiss LSM 510 confocal microscope equipped with C-Apochromat 40×/1.2 W water-immersion objective using the 488 nm line of an argon laser and/or the 543 nm line of a HeNe laser at 25 °C. Cell borders were outlined from differential interference contrast images.

Images of 30–40 polarized cells expressing Cav-1-GFP were randomly recorded. Green fluorescence intensity in six regions (three at the cell front and three at the cell rear; see Fig. 2*B*) of each cell was measured using Image J software. Cav-1 depolarization was assumed if a ratio of rear-to-front fluorescence intensity was equal to or less than the cells expressing GFP. If a ratio of rear-to-front fluorescence intensity of a Cav-1 mutant was significantly higher than the cells expressing GFP but less than wild-type Cav-1 ($Cav_{1–178}$-GFP), a partial polarization was assumed. We have shown that loss of Cav-1 polarity affects cell polarization (24). In the present study, we focused only on the polarized subpopulation of the cells to determine the polarity of Cav-1 mutants (see "Results").

Immunoprecipitation and Immunoblot Analysis—$Cav_{61–178}$-GFP or $Cav_{61–178}$-FLAG was expressed in Cav-$1^{-/-}$ MEFs, and the cells were lysed in ice-cold lysis buffer containing 1% Triton X-100, 0.5% Nonidet P-40, 60 mM octylglucoside, 1 mM EGTA, and 10 mM Tris-HCl (pH 7.4) supplemented with protease inhibitors. The lysates were precleared and immunoprecipitated with polyclonal GFP antibodies or monoclonal anti-FLAG M2 antibodies at 4 °C. Immunoprecipitates were boiled for 4 min in Laemmli sample buffer. The samples were separated by SDS-PAGE on a 12% gel, electrotransferred to a nitrocellulose membrane, and immunoblotted against Cav-1. Bands were visualized by SuperSignal West Pico chemiluminescent substrate (Pierce).

Purification of Caveolin-rich Membrane Domains—Caveolin-rich membrane domains were isolated as described previously (29). In brief, confluent cells were scraped into sodium carbonate (pH 11.0) and homogenized. The resulting homogenate was mixed with the same volume of 90% sucrose in MES-buffered saline, which was overlaid by 35 and 5% sucrose in MES-buffered saline. The gradient was then centrifuged at 39,000 rpm for 16 h in an SW41 rotor, and then 12 fractions of 1 ml in each were collected, starting from the top of the gradient, for immunoblot analysis.

Transmission Electron Microscopy—Cav-$1^{-/-}$ MEFs were infected with or without $AdCav_{1–178}$ or $AdCav_{61–178}$. Twenty-four hours post-infection, cells were seeded onto gelatin-coated dishes, fixed with 4% paraformaldehyde and 0.25% glutaraldehyde in phosphate buffer, and scraped into a microcentrifuge tube. The samples were post-fixed with osmium tetroxide and then embedded in epon. The sections were stained with uranyl acetate and lead citrate. Thin sections of samples were examined under a JEOL 1220 transmission electron microscope.

RESULTS

Deletion of aa 1–60 at the N Terminus Prevents Rear Polarization of Caveolin-1—Upon cell migration, Cav-1 is excluded from the leading edge and polarized to the cell rear. On the basis of previous extensive studies to identify domains that dictate caveolin intracellular trafficking, we reasoned that when cells are stimulated to migrate, Cav-1 moves to the rear of migrating cells in a sequence-specific fashion as a mechanism to sequester it away from signaling proteins that direct lamellipod protrusion. To determine the amino acid sequence that is necessary for Cav-1 polarization, we started by generating a series of caveolin-1 mutants by deletion mutations across the molecule, because this strategy had been used successfully to characterize domains for caveolar membrane targeting and intracellular trafficking (22, 23, 30–32). To assess the trafficking of Cav-1 mutants, we chose Cav-$1^{-/-}$ cells that were deficient in endogenous Cav-1 and would not sequester the mutants and keep them from depolarizing (see Fig. 3). The deletion mutants used in the present study include $Cav_{32–178}$, $Cav_{61–178}$, and $Cav_{1–156}$ (Fig. 1). Previous studies have shown that deletion of aa 60–80 results in trapping the molecule in the endoplasmic reticulum (ER), whereas deletion of either aa 80–100 or 134–154 leads to co-localization with a Golgi marker (22). Thus, Cav-1 mutants that have been shown previously to sort improperly after expression were excluded from the present study. Wild-type and mutant Cav-1 generated as GFP fusion proteins were transiently expressed in Cav-$1^{-/-}$ MEFs and detected in a punctate pattern on the plasma membrane and, to a lesser extent, in the perinuclear regions (apparently the Golgi apparatus) in stationary cells (data not shown).

Our previous study showed that targeted knockdown of Cav-1 using Cav-1 siRNA (small interfering RNA) impeded human endothelial cell polarization by 3-fold and inhibited cell directional movement (24). This result was confirmed by our recent study demonstrating a dramatic decrease in the number of polarized mouse pulmonary endothelial cells from 32 ± 3.8% in wild-type cells to 16 ± 3.5% in Cav-$1^{-/-}$ cells ($p < 0.01$), suggesting that Cav-1 polarity plays an important role in cell

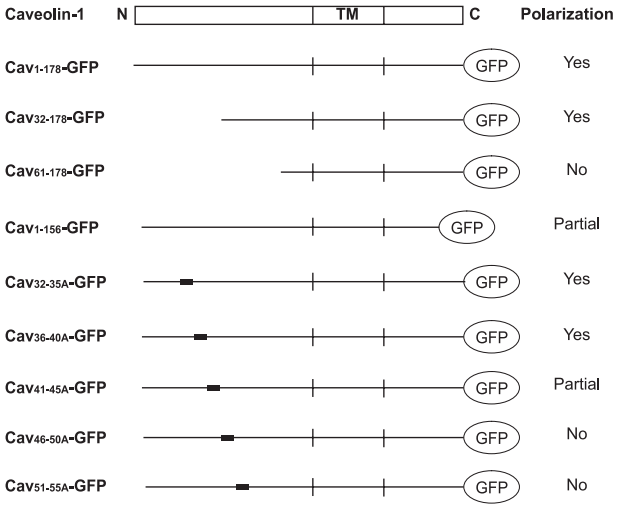

FIGURE 1. **Schematic representation of wild-type and mutant Cav-1.** Nine different Cav-1 constructs were used in this study. Cav-1 is divided into three domains. The N terminus (residues 1–101) and C terminus (residues 135–178) are separated by a hydrophobic transmembrane domain (*TM*; residues 102–134). Full-length and mutant Cav-1 were fused with GFP. The location of the alanine substitutions in each construct (Cav_{32-35A}-GFP to Cav_{51-55A}-GFP) is indicated by a *black box*. The ability of the constructs to polarize in migrating Cav-$1^{-/-}$ MEFs is indicated in the column to the *right* of each construct.

polarization. Although the number of polarized cells was dramatically reduced, some Cav-1 depolarized cells were able to polarize, suggesting that Cav-1 depolarization was not sufficient to completely block cell polarization. Thus, we expected that ectopic expression of full-length Cav-1 in Cav-$1^{-/-}$ cells would restore cell polarization and that expression of Cav-1 mutants would impede cell polarization and, subsequently, the polarity of the Cav-1 mutants. Therefore, in the present study, we focused only on the polarized subpopulation of cells to determine the polarity of Cav-1 mutants.

Consistent with previous observations (24, 25), Cav_{1-178}-GFP polarized at the rear of migrating Cav-$1^{-/-}$ MEFs (Fig. 2*A*, *a*), suggesting that exogenously expressed Cav-1 behaves as endogenous protein and is able to polarize in Cav-1-deficient cells. Deletion of aa 1–31 retained Cav-1 rear polarity. In contrast, deletion of aa 1–60 (Cav_{61-178}-GFP) prevented rear polarization of the protein, and instead signals of the mutant were detected at the leading edge (Fig. 2*A*, *d*), suggesting that aa 32–60 are necessary for Cav-1 polarization.

To assess whether the C-terminal domain plays a role in Cav-1 polarization, Cav-$1^{-/-}$ MEFs were transfected with a Cav-1 mutant lacking the final 22 amino acids (Cav_{1-156}-GFP). As shown in Fig. 2*A*, *c*, the mutant polarized at the cell rear. In addition, weak signals were detected at the cell front, suggesting a partial polarization of the mutant.

To analyze the polarized Cav-1-GFP signal statistically in migrating cells, fluorescence intensity in six regions (three at the cell front and three at the cell rear; see Fig. 2*B*) was detected, and a ratio of rear-to-front fluorescence intensity was determined in each mutant ($n \geq 30$) (see "Experimental Procedures") and compared with GFP only. Statistical analysis revealed that the ratio of rear-to-front fluorescence intensity in Cav_{1-178}-GFP- or Cav_{32-178}-GFP-expressing cells was 2.6- or 2.3-fold more than that in GFP, respectively ($p < 0.0001$; Table 1, Fig. 2*C*), suggesting that deletion of the first 31 aa at the N

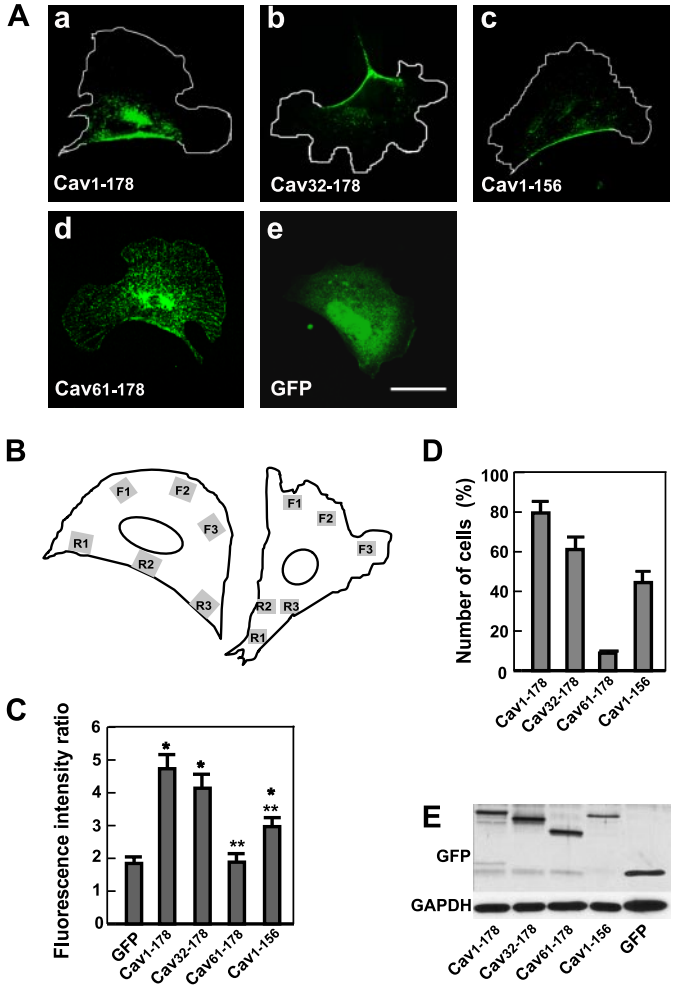

FIGURE 2. **Deletion of the N terminus of Cav-1 prevents polarization of the protein.** *A*, Cav-$1^{-/-}$ MEFs were transfected with the constructs expressing Cav_{1-178}-GFP (*a*), Cav_{32-178}-GFP (*b*), Cav_{1-156}-GFP (*c*), Cav_{61-178}-GFP (*d*), or GFP alone (*e*). Twenty-four hours post-transfection, cells were seeded to allow migration, fixed with 2% paraformaldehyde and examined by confocal fluorescence microscopy (*a–c*, cell borders are *outlined* by a *white line*). Note that Cav_{1-178}-GFP (*a*) and Cav_{32-178}-GFP (*b*) polarize in Cav-$1^{-/-}$ MEFs. In contrast, deletion of the first 60 amino acids at the N terminus (*d*) prevents the protein from polarization, and the mutant signal is detected at the leading edge. *Scale bar*, 20 μm. *B* and *C*, images of polarized cells expressing either full-length or mutant Cav-1 were randomly recorded, and the fluorescence intensity in six regions (three at the cell front (*F1–F3*) and three at the cell rear (*R1–R3*)) (*B*) was measured as described under "Experimental Procedures." A ratio of rear-to-front fluorescence intensity in each mutant was determined (*C*). Data are the mean ± S.E. from three independent experiments. Statistical analysis is shown in Table 1. *, $p < 0.01$ compared with GFP only; **, $p < 0.01$ with full-length Cav-1 (Cav_{1-178}-GFP). *D*, the number of Cav-1 polarized cells was determined by comparing the ratio of rear-to-front fluorescence intensity in each mutant with that of GFP. Polarization of a Cav-1 mutant was assumed if fluorescence intensity ratio of the mutant was higher than 2 S.D. of the mean of GFP. Data are the mean ± S.E. from three independent experiments. *E*, a parallel set of the cells transfected with the constructs described in *A* were lysed, and the lysates were subjected to SDS-PAGE and Western blotting with antibody for GFP and GAPDH.

TABLE 1

Student's *t* test analysis of the fluorescence intensity of Cav-1 deletion mutants

Construct	*p* value compared with Cav_{1-178}-GFP	*p* value compared with GFP
Cav_{1-178}-GFP		6.640×10^{-9}
Cav_{32-178}-GFP	0.276	1.540×10^{-6}
Cav_{61-178}-GFP	8.858×10^{-9}	0.724
Cav_{1-156}-GFP	2.016×10^{-4}	5.407×10^{-5}

terminus does not affect the polarity of the protein. In contrast, deletion of an additional 29 aa dramatically reduced the fluorescence intensity ratio to the level of GFP, suggesting loss of polarity (Fig. 2*C*). The fluorescence intensity ratio in Cav_{1-156}-GFP was 1.6-fold higher than GFP ($p < 0.01$) but 1.6-fold lower than Cav_{1-178}-GFP ($p < 0.01$), indicating partial polarization (Table 1; Fig. 2*C*). The effect of deletion mutation on Cav-1 polarization was not due to protein expression levels (Fig. 2*E*).

The number of Cav-1-polarized cells expressing each construct was determined by comparing the ratio of rear-to-front fluorescence intensity in each mutant with that of GFP. As described above, we focused only on the polarized subpopulation of the cells. Polarization of a Cav-1 mutant was assumed if fluorescence intensity ratio of the mutant was more than 2 S.D. of the mean of GFP. Fig. 2*D* shows that 79.5 ± 5.7% of morphologically polarized cells expressing full-length Cav-1 display Cav-1 rear polarization. In contrast, up to 8.8 ± 0.25% of polarized cells expressing Cav_{61-178}-GFP show rear polarization. The number of Cav-1 rear polarization cells is 44 ± 5.5% of polarized cells expressing the partial polarity mutant, Cav_{1-156}-GFP.

Cav_{61-178}-GFP Regains Polarity by Interacting with Endogenous Caveolin-1—Cav-1 exists as a high molecular mass in living cells, which is mediated by the oligomer domain, aa 61–101 (33). It is possible that expression of the depolarization mutant Cav_{61-178}-GFP would affect the localization of endogenous Cav-1 in a migrating cell. To test this hypothesis, we expressed Cav_{61-178}-GFP in either HUVECs or wild-type MEFs known to express Cav-1 and examined the localization of endogenous Cav-1 using polyclonal antibody for Cav-1 (the antibody recognizes an epitope at the N terminus of Cav-1 and does not react with our depolarization mutant). Fig. 3*A* shows that the depolarization mutant Cav-1 is co-localized with endogenous Cav-1, and interestingly, the mutant is polarized together with wild-type Cav-1 at the cell rear. This result suggests that the mutant may be trapped and co-translocated with endogenous Cav-1 to the rear of migrating cells.

To assess whether the mutant interacted with endogenous Cav-1, wild-type MEFs were transfected with or without the depolarization construct expressing Cav_{61-178}-GFP and subjected to immunoprecipitation with specific antibody for GFP. As shown in Fig. 3*B*, endogenous Cav-1 is co-precipitated with Cav_{61-178}-GFP (monoclonal antibody (clone 2297) recognizes an epitope within aa 61–71 (34), and reacts with the depolarization mutant, Cav_{61-178}-GFP). To confirm this result, we generated an adenovirus harboring FLAG-tagged mutant Cav-1 (Cav_{61-178}-FLAG). Wild-type MEFs were infected with the adenovirus and subjected to immunoprecipitation with an antibody specific for FLAG. Again, endogenous Cav-1 was detected in the immunoprecipitation complex (Fig. 3*B*), suggesting an interaction between the mutant and endogenous Cav-1.

Caveolin-1 is a principal protein component of caveolar membranes and resists solubilization in nonionic detergents at cold temperatures (35, 36). This physical property reflects enrichment of cholesterol and glycosphingolipids in caveolae (17). To determine whether Cav_{61-178} was tightly associated with lipid rafts, HUVECs were infected with $AdCav_{61-178}$ and extracted with alkaline sodium carbonate, an agent that strips

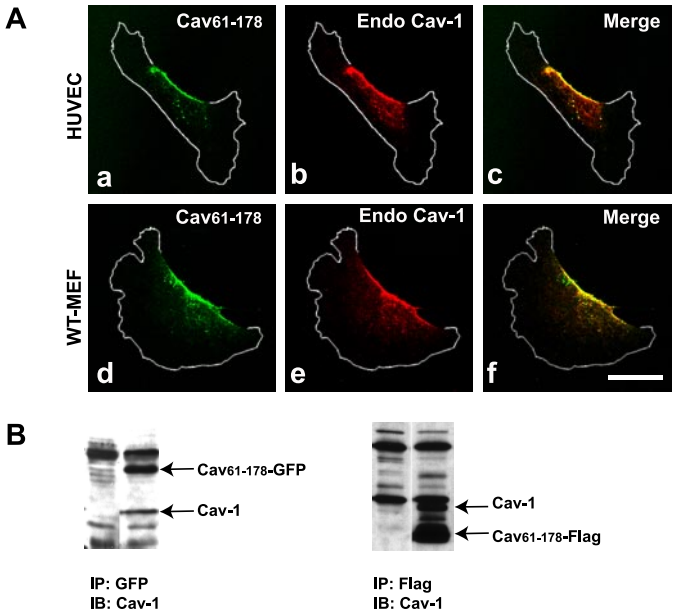

FIGURE 3. **Cav_{61-178}-GFP becomes polarized in cells expressing endogenous Cav-1.** *A*, HUVECs (*a–c*) or wild-type MEFs (*d–f*) were transfected with a construct expressing Cav_{61-178}-GFP. Twenty-four hours post-transfection, cells were seeded to allow migration, fixed, and stained with antibody for Cav-1 followed by rhodamine Red-X-conjugated secondary antibody. Note that Cav_{61-178}-GFP (*a* and *d*) is co-localized with endogenous Cav-1 and becomes polarized in HUVECs as well as wild-type MEFs. *Scale bar* = 20 μm. *B*, wild-type MEFs were transfected with a construct expressing Cav_{61-178}-GFP (*a*) or infected with adenovirus harboring FLAG-tagged Cav_{61-178} (Cav_{61-178}-Flag) (*b*). After 24 h, cells were lysed, and the lysates were subjected to immunoprecipitation (*IP*) with antibody for either GFP or FLAG followed by SDS-PAGE and immunoblotting (*IB*) with specific antibody for Cav-1.

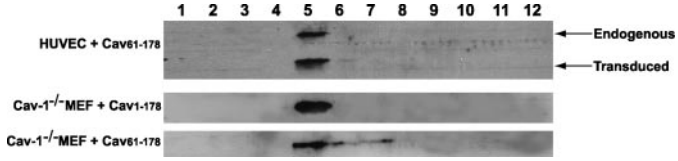

FIGURE 4. **Association of Cav_{61-178} with caveolin-rich membrane domains.** Twenty-four hours post-infection of HUVECs with adenovirus harboring Cav_{61-178} ($AdCav_{61-178}$) or Cav-$1^{-/-}$ MEFs with either $AdCav_{1-178}$ or $AdCav_{61-178}$, low density membrane domains were isolated using a detergent-free method (see "Experimental Procedures"). After sucrose gradient ultracentrifugation, 12 fractions were collected. Equal volume aliquots of each fraction were subjected to SDS-PAGE and immunoblotted with specific antibody for Cav-1. Note that Cav_{61-178} is co-fractionated with endogenous Cav-1 at fraction 5 from HUVECs. In Cav-$1^{-/-}$ MEFs, Cav_{61-178} is targeted to the light density membrane domains.

membranes of peripherally associated proteins, followed by an established sucrose density centrifugation method to purify caveolae microdomains (37, 38). Fig. 4 shows that Cav_{61-178} is co-fractionated with endogenous Cav-1 (*fraction 5, top panel*). To assess whether the association with caveolae membranes resulted from its interaction with endogenous Cav-1, Cav-$1^{-/-}$ MEFs were infected with either $AdCav_{1-178}$ or $AdCav_{61-178}$, and caveolae were isolated. We found that most of the mutant protein was recovered in *fractions 5–7*, indicating an integration of the mutant itself into lipid rafts (Fig. 4, *lower panel*).

Deletion of aa 1–60 Impedes Caveolae Formation—Cav-1 is a known critical factor required for biogenesis of caveolae. Cav-1 is a cholesterol-binding protein and may facilitate the concentration of a critical mass of cholesterol required for caveolae

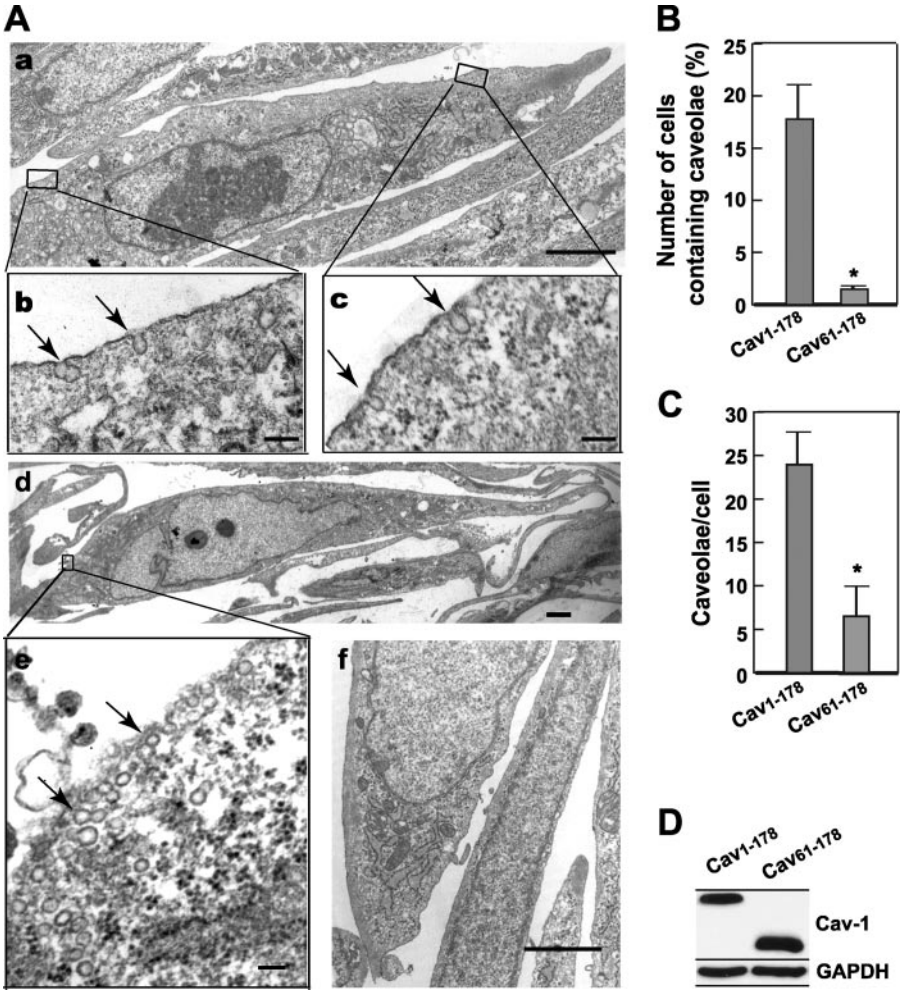

FIGURE 5. **Deletion of aa 1–60 impedes caveolae formation.** *A*, Cav-1$^{-/-}$ MEFs were infected with either AdCav$_{61-178}$ (*a–c*) or AdCav$_{1-178}$ (*d* and *e*) or were mock infected (*f*). Twenty-four hours post-infection, cells were fixed and processed for transmission electron microscopy. As expected, there was no caveolar structure in Cav-1$^{-/-}$ cells (*f*). In contrast, transduced expression of wild-type Cav-1 (*d* and *e*) resulted in caveolae formation (*arrows*). Interestingly, deletion of the first 60 aa led to a dramatic reduction in caveolae formation (*arrows* in *a–c*). *b*, *c*, and *e* are images at higher magnification of images *a* and *d*, respectively. *Scale bars*: 100 nm for *b*, *c* and *e*; 2 μm for *a*, , and *f*. *B* and *C*, images were randomly recorded; 90 (AdCav$_{1-178}$-infected) or 198 (AdCav$_{61-178}$-infected) cells were viewed. The number of cells that contained caveolae (*B*) and the number of caveolae in each cell (*C*) were counted. Data are the mean ± S.E. from three independent experiments. *, $p < 0.05$. *D*, 24 h post-infection, a parallel set of cells was lysed and subjected to SDS-PAGE and Western blotting with antibody for Cav-1. The same membrane was reprobed with antibody for GAPDH to show equal protein loading.

depolarized in cells expressing the depolarization mutant, Cav-1$^{-/-}$ MEFs were infected with adenovirus harboring either wild-type (AdCav$_{1-178}$) or the mutant Cav-1 (AdCav$_{61-178}$) and processed for transmission electron microscopy. Fig. 5*A* shows that expression of wild-type Cav-1 induces caveolae formation, which localizes abundantly at the rear of a migrating cell as we have demonstrated previously (24). Surprisingly, expression of the depolarization mutant Cav-1 dramatically decreased the number of cells that were induced to form caveolae, by more than 12-fold (Fig. 5*B*). Furthermore, the number of caveolae in each cell was dramatically decreased by up to 4-fold (Fig. 5*C*). The impairment of caveolae formation did not result from protein expression levels (Fig. 5*D*). Because few caveolae were formed by the depolarization mutant, we were not able to determine whether caveolae were polarized in these cells.

Identification of the Minimal Amino Acid Sequence Required for Caveolin-1 Polarization—Our results thus indicate that aa 32–60 are critical for the rear polarization of Cav-1. To identify the minimal sequence that is necessary for Cav-1 polarization, we generated a series of consecutive quadro- or penta-alanyl codon substitutions from aa 32 to 55 (Fig. 1) and examined the localization of the mutants by fluorescence microscopy (Fig. 6). Substitution of aa 32–40 with alanine (Cav$_{32-35A}$-GFP, Cav$_{36-40A}$-GFP) did not affect Cav-1 polarity (Fig. 6*A*, *a* and *b*). Substitution of aa 41–45 with alanine (Cav$_{41-45A}$-GFP) led to partial polarization of Cav-1 (*c* in Fig. 6*A*). In clear contrast, replacement of aa 46–55 with alanine (Cav$_{46-50A}$-GFP, Cav$_{51-55A}$-GFP) prevented the rear polarization of Cav-1 (Fig. 6*A*, *d* and *e*).

Statistical analysis revealed that the ratio of rear-to-front fluorescence intensity in Cav$_{46-50A}$-GFP- and Cav$_{51-55A}$-GFP-expressing cells was similar to GFP but was reduced by 3-fold compared with full-length Cav-1 (Cav$_{1-178}$-GFP) ($p < 0.0001$) (Table 2; Fig. 6*B*). The fluorescence intensity in Cav$_{41-45A}$-GFP was about 1.5-fold higher than GFP ($p < 0.05$) but 2-fold lower than Cav$_{1-178}$-GFP ($p < 0.0001$), indicating partial polarization (Table 2; Fig. 6*B*). Thus, we have identified a sequence motif in Cav-1, ^{46}TKEIDLVNRD^{55}, that is essential for the rear polarization of the protein in migrating cells. The effect of alanine

invagination. Overexpression of Cav-1 in a lymphocytic cell line that does not endogenously express the protein and lacks caveolae is sufficient to induce the formation of caveolae (39). Genetic ablation of Cav-1 generates animals that lack caveolae (40, 41).

Upon the discovery of their abundance in endothelium, caveolae have been postulated as vesicular carriers mediating endocytosis and transcytosis (7, 42). Indeed, caveolae have the molecular transport machinery for vesicle budding, docking, and fusion (43). Thus, at least in endothelium, caveolae may integrate signaling events with vesicular transport (44). We and others have shown that concomitant with Cav-1 polarization, caveolae move to cell posterior as well (24, 25), suggesting that caveolae may function as transport cargos carrying Cav-1 to cell rear. To test whether aa 1–60 of Cav-1 affect caveolae formation and whether caveolae are

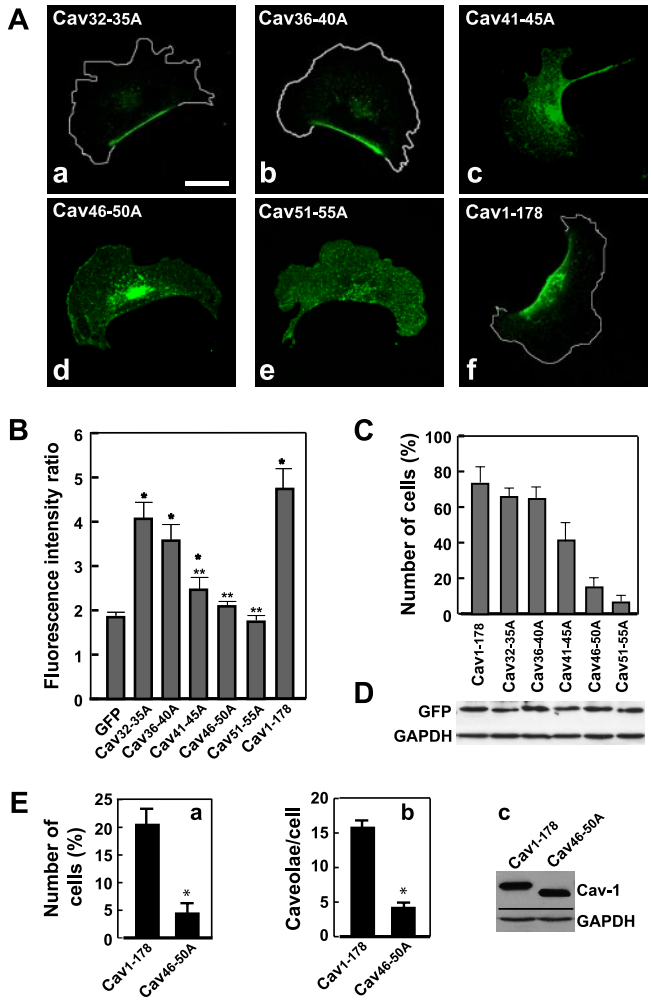

FIGURE 6. **Amino acids 46–55 are required for Cav-1 rear polarization.** *A*, Cav-1$^{-/-}$ MEFs were transfected with constructs with a series of consecutive quatra- or penta-alanine substitutions between aa 32 and 55 of Cav-1. Twenty-four hours post-transfection, cells were seeded to allow migration, fixed, and examined by confocal fluorescence microscopy (*a*, *b*, and *f*, cell borders are *outlined* in *white*). Note that substitution of amino acids 46–50 or 51–55 (*d* and *e*) with alanine prevents Cav-1 polarization. *Scale bar*, 20 μm. *B*, images of polarized cells expressing Cav-1 mutants ($n \geq 30$ for each construct) were randomly recorded. Fluorescence intensity in six regions was measured, and a ratio of rear-to-front fluorescence intensity in each mutant was determined as described in the legend to Fig. 2*B*. Data are the mean ± S.E. from three independent experiments. Statistical analysis is shown in Table 2. *, $p < 0.05$ compared with GFP only; **, $p < 0.01$ with full-length Cav-1 (Cav_{1-178}-GFP). *C*, the number of Cav-1 polarized cells was determined as described in the legend to Fig. 2. Data are the mean ± S.E. from three independent experiments. *D*, a parallel set of the cells transfected with the constructs as in *A* was lysed, and the lysates were subjected to SDS-PAGE and Western blotting with antibody for GFP and GAPDH. *E*, Cav-1$^{-/-}$ MEFs were infected with either $AdCav_{1-178}$ or $AdCav_{46-50A}$. Twenty-four hours post-infection, cells were fixed and processed for transmission electron microscopy. Images were randomly recorded; 40 ($AdCav_{1-178}$-infected) or 68 ($AdCav_{46-50A}$-infected) cells were viewed. The number of cells that contained caveolae (*a*) and the number of caveolae in each cell (*b*) were counted. Data are the mean ± S.E. from two independent experiments. *, $p < 0.05$. Twenty-four hours post-infection, a parallel set of cells was lysed and subjected to SDS-PAGE and Western blotting with antibody for Cav-1 (*c*). The same membrane was reprobed with antibody for GAPDH to show equal protein loading.

substitution on Cav-1 polarization was not due to protein expression levels (Fig. 6*D*).

The number of Cav-1-polarized cells expressing each construct was determined as described above. Polarization of a Cav-1 mutant was assumed if the fluorescence intensity ratio of the mutant was more than 2 S.D. of the mean of GFP. Fig. 6*C* shows that about 65% of the polarized cells expressing Cav_{32-35A}-GFP or Cav_{36-40A}-GFP display Cav-1 rear polarization. In contrast, about 15% of the polarized cells expressing Cav_{46-50A}-GFP or 6.4% of the polarized cells expressing Cav_{51-55A}-GFP show rear polarization. The number of Cav-1 rear polarization cells is about 41% of polarized cells expressing Cav_{41-45A}-GFP.

TABLE 2
Student's *t* test analysis of the fluorescence intensity of alanine replacement mutants

Construct	*p* value compared with Cav_{1-178}-GFP	*p* value compared with GFP
Cav_{32-35A}-GFP	0.226	3.215×10^{-6}
Cav_{36-40A}-GFP	0.203	8.150×10^{-6}
Cav_{41-45A}-GFP	3.799×10^{-6}	0.016
Cav_{46-50A}-GFP	2.629×10^{-8}	0.135
Cav_{51-55A}-GFP	3.935×10^{-9}	0.392

To assess whether the alanine substitution mutants affect caveolae formation, Cav-1$^{-/-}$ MEFs were infected with adenovirus harboring either wild-type ($AdCav_{1-178}$) or an alanine substitution of aa 46–50 mutant ($AdCav_{46-50A}$) and processed for transmission electron microscopy. As shown in Fig. 6*E*, substitution of aa 46–50 with alanine dramatically decreased (by 5-fold) the number of cells that were induced to form caveolae (Fig. 6*E*, *a*). Furthermore, the number of caveolae in each cell was dramatically decreased by 3.5-fold (Fig. 6*E*, *b*). The impairment of caveolae formation did not result from protein expression levels (Fig. 6*E*, *c*). Thus, these results suggest that aa 46–50 play important role in Cav-1 polarity and caveolae formation.

Loss of Caveolae Fails to Prevent Cav-1 Polarization—The observation that mutation of aa 46–50 coincidentally blocked Cav-1 polarization as well as caveolae formation is interesting and suggests that: 1) Cav-1 polarity is caveolae-dependent, or 2) the sequence motif is required both for Cav-1 polarization and caveolae formation. To test these hypotheses, we employed an alternative model by treating wild-type MEFs with MβCD to reduce cellular cholesterol level, which is known to block caveolae formation (45) and disperse Cav-1 in the plasma membranes (27). In the absence of MβCD, more than 50% of the MEFs examined showed caveolae structure, and the number of caveolae in those cells was about 14 caveolae/cell. Treatment of the cells with 10 mM MβCD dramatically suppressed the number of cells containing caveolae by more than 3.5-fold and the number of caveolae by 4.5-fold (Fig. 7*A*). However, the loss of caveolae formation failed to prevent Cav-1 rear polarization (Fig. 7, *B* and *C*). Thus, these results suggest that a caveolae-independent mechanism may mediate Cav-1 rear polarization.

Caveolin-1 Polarity Plays an Important Role in Cell Directional Movement—The generation of Cav-1 null cells provided a genetic model of Cav-1 depolarization and was used to test their ability to migrate directionally toward chemoattractant (10% FBS) using a well characterized chemotaxis Dunn chamber (28). In this system, cells were viewed directly and recorded over a 6-h period by a live cell time-lapse imaging system. Only cells migrating at least 20 μm (the "horizon" distance) were included in the calculation (see "Experimental Procedures"). Cell trajectories from three independent experiments were tracked manually, converted to a set of angular directions, and

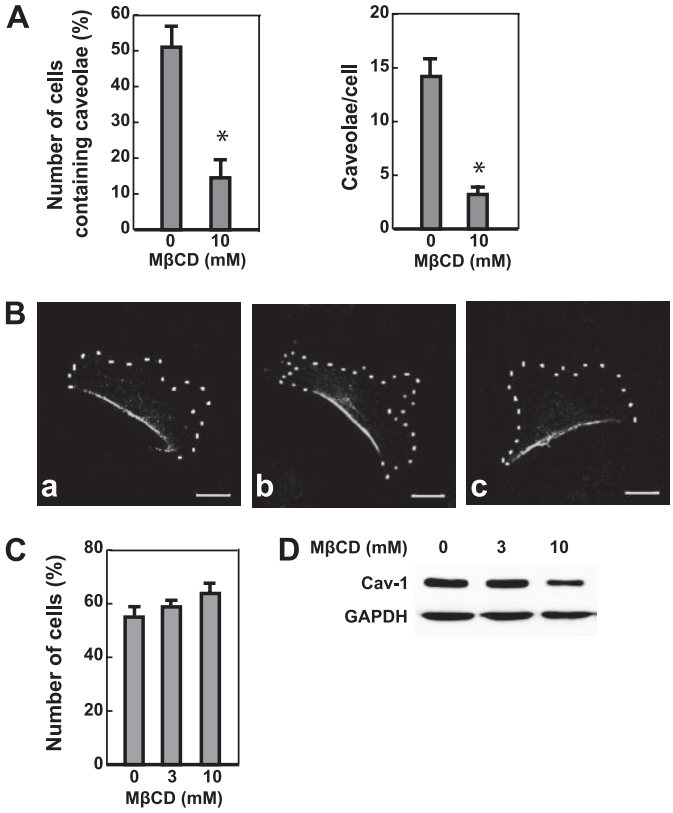

FIGURE 7. **Knockdown of caveolae does not affect Cav-1 polarity.** *A*, wild-type MEFs were treated with 0 or 10 mM MβCD for 30 min, fixed, and then processed for transmission electron microscopy. The number of cells containing caveolae and the number of caveolae in those cells were counted. Note that MβCD treatment dramatically reduces caveolae numbers. Data are the mean ± S.D. *, $p < 0.05$. *B* and *C*, after treatment with 0 (*a*), 3 (*b*), or 10 (*c*) mM MβCD, wild-type MEFs were fixed and stained with antibody for Cav-1 (*B*). *Dotted lines* indicate cell borders. Images were randomly recorded, and the number of Cav-1 polarized cells was counted (*C*). Note that knockdown of caveolae by MβCD does not affect Cav-1 polarization. Data are the mean ± S.D. *D*, a parallel set of the cells pretreated with MβCD as described in *B* was lysed, and cell lysates were subjected to SDS-PAGE and Western blot analysis with antibody for Cav-1.

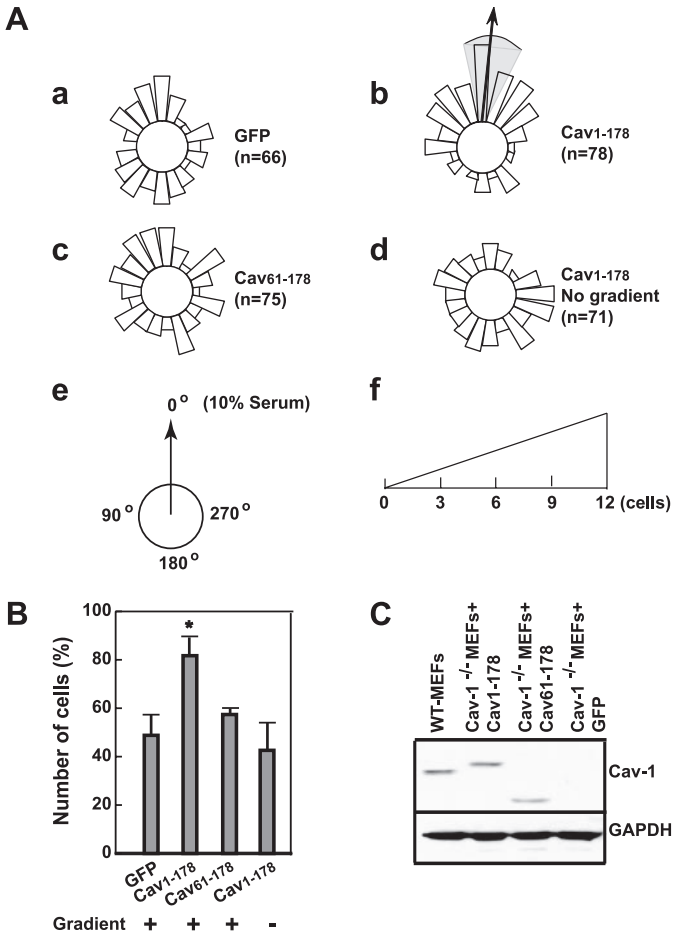

FIGURE 8. **Caveolin-1 polarity plays an important role in cell directional movement.** *A*, Cav-1$^{-/-}$ MEFs were infected with adenovirus expressing GFP only (AdGFP) (*a*), full-length Cav-1 ($AdCav_{1-178}$) (*b* and *d*), or the depolarization mutant ($AdCav_{61-178}$) (*c*). The directional migration of the cells was analyzed using a chemotaxis Dunn chamber. Cells were exposed to either a gradient from 0.25% to 10% FBS (*a–c*) or no gradient (0.25% FBS in both chambers) (*d*). The direction of the gradient is indicated by the *arrow* in *e*. The data are presented as a *circular histogram* in which the length of each 18° segment (as shown in *f*) represents the number of cells with an average angle of migration falling within that particular interval (see "Experimental Procedures"). The mean direction of chemotaxis is displayed as an *arrow*, and the 95% confidence interval as a *gray arc*. *B*, quantitative analysis of cell directional movement. The number of chemotactic cells was determined by counting the cells with net movement toward serum gradient (these include the cells in the segments between 0 and 90° and 270 and 360° (see *A*, *panel e*). Note that Cav-1$^{-/-}$ MEFs expressing GFP or the depolarization mutant show negligible chemotactic movement. Data are the mean ± S.D. *, $p < 0.05$ compared with GFP. *C*, Cav-1$^{-/-}$ MEFs were infected with $AdCav_{1-178}$, $AdCav_{61-178}$, or AdGFP. Twenty-four hours post-infection, cells were lysed, and the lysates were subjected to SDS-PAGE and immunoblotting with antibody for Cav-1. The same membrane was reprobed with antibody for GAPDH to show equal protein loading. *WT*, wild type.

displayed in a circular histogram (Fig. 8*A*). The majority of Cav-1-deficient cells demonstrated disorientated migration (Fig. 8*A*, *a*). To test the effect of the depolarization mutant Cav-1 on chemotaxis, we infected Cav-1$^{-/-}$ MEFs with the adenovirus harboring full-length Cav-1 (Cav_{1-178}), the depolarization mutant Cav-1 (Cav_{61-178}), or GFP only. The expression levels of the full-length and the depolarization mutant Cav-1 were similar to the level of wild-type MEFs (Fig. 8*C*). Interestingly, expression of full-length Cav-1 in the Cav-1$^{-/-}$ cells resulted in up-gradient directional migration (Fig. 8*A*, *b*). In contrast, expression of the depolarization mutant, Cav-1, was not able to rescue the disoriented migration of the Cav-1$^{-/-}$ cells (Fig. 8*A*, *c*), thus suggesting that the rear polarization of Cav-1 plays an important role in chemotaxis. Quantitative analysis shows that expression of full-length Cav-1 caused more than 80% cells to migrate toward serum, whereas cells expressing GFP or the depolarization mutant showed negligible chemotactic movement (Fig. 8*B*).

DISCUSSION

Cell migration involves the asymmetrical organization of plasma membrane features that are associated with the cytoskeleton and signaling molecules. We and other groups have recently shown that Cav-1 was specifically polarizes to the posterior of migrating cells (22, 24, 25). In the present study, we systematically identified and characterized a domain at the N terminus of Cav-1 that controls rear polarization of the protein. Previous studies have identified a number of functional elements in caveolin. These include identification of the caveolin scaffolding domain that interacts with multiple signaling molecules (46, 47); the segment that is involved in self-association to form oligomers (33); the Golgi and ER localization signals (22, 23); the caveolin-inhibitory domain that inhibits endothe-

lial nitric-oxide synthase, c-Src, and protein kinase A (48, 49); and the N- and C-terminal membrane attachment domains (31, 32). These investigations have employed cell systems that express endogenous Cav-1. Evidence has shown that interaction between the transduced and endogenous Cav-1 may mask crucial trafficking information (Ref. 50 and our present study on HUVECs and wild-type MEFs). The success of the present study depended on employing a cell system that was genetically deficient in Cav-1. Using this system, we have identified a sequence motif, aa 46–55, that is essential for Cav-1 rear polarization and caveolae formation in migrating cells.

The observations that deletion of aa 1–60 or mutation of aa 46–50 coincidentally blocked Cav-1 polarization as well as caveolae formation suggest that Cav-1 polarity may be caveolae-dependent. This idea is consistent with caveolae functioning as transport cargos carrying Cav-1 to the rear of the cell. Thus, the mutation-induced Cav-1 depolarization may be indirect and may result from a loss of caveolae structure. We tested this hypothesis by depletion of cholesterol to block caveolae formation (45) and found that loss of caveolae failed to prevent the polarization of endogenous full-length Cav-1. Taken together, our results suggest that Cav-1 polarity appears to be mediated by 1) caveolae and/or 2) a sequence motif at the N terminus of the protein.

Multiple sequence alignment of Cav-1, -2, and -3 shows that the sequence from aa 47 to 56 is 100% identical between Cav-1 and Cav-3 (16), suggesting that this segment may mediate common functions shared by the two proteins. Another N-terminal conserved sequence, designed as the signature domain, is aa 68–75, which contains the sorting signal (aa 66–70) responsible for exit from the ER (22). The sequence of aa 46–55 does not resemble any domain with known function. Thus, the conserved sequence represents a novel domain that dictates subcellular translocation of Cav-1. We propose the term N-CPD (N-terminal caveolin polarity domain). The N-terminal (aa 1–79) and C-terminal (122–178) tails of Cav-1 are believed to be unstructured hydrophilic tails that remain entirely cytosolic and are accessible for cytosolic protein interactions (16). Thus, N-CPD might interact with an unidentified factor(s) that controls Cav-1 polarization in migrating cells.

When expressed either in HUVECs or wild-type MEFs that express endogenous Cav-1, deletion of N-CPD failed to prevent the mutant Cav-1 from polarization. This was not surprising, given the nature of caveolin and caveolin self-interaction (via aa 61–101) to form homo-oligomers before incorporation into glycosphingolipid-rich membranes in the Golgi apparatus (19). Indeed, our present results show that the depolarization mutant co-localizes and interacts with endogenous Cav-1. These results are consistent with previous observations indicating that the deletion and alanine substitution mutants retain the same orientation with wild-type Cav-1, have relatively normal confirmation, and are not shunted into a degradation pathway (22). Furthermore, the mutant is tightly associated with lipid rafts. Surprisingly, deletion of aa 1–60 or mutation of aa 46–50 dramatically impeded caveolae formation. This was likely not caused by the interruption of the binding between Cav-1 and cholesterol, because this mutant contains the putative free cholesterol-binding sequence (^{94}**V**TK**Y**WFY**R**^{101}) (51). The results suggest that aa 46–50 may play a role in caveolae formation.

In the present study, we found that when expressed in MEFs, the majority signals of our depolarization mutant, Cav_{61-178}-GFP, which lacked the first 60 aa, localized in a punctate pattern on the plasma membrane and, to a lesser extent, in the Golgi apparatus. Similarly, Machleidt *et al.* (22) recently showed plasma membrane targeting of the same mutant that lacked the first 59 aa, Cav_{60-178}, when it was expressed in CHO cells. A recent study showed that expression of a deletion mutant that lacked the first half of the N-terminal domain (aa 3–48) in Fischer rat thyroid cells resulted in the accumulation of the mutant in the Golgi apparatus, although it oligomerized normally and associated with lipid rafts (30). The difference apparently resulted from the cell types used for protein expression. For instance, Fischer rat thyroid cells are likely to exhibit more pronounced Golgi apparatus staining of ectopically expressed proteins, such as full-length Cav-1, than other types of the cells that express Cav-1 endogenously, suggesting that Fischer rat thyroid cells are more sensitive to the conformational changes of Cav-1 (52).

Mutagenesis and biochemical analysis suggest that Cav-1 is cycling between caveolae and intracellular compartments. The transport depends on critical elements in the molecule required for the proper targeting to intracellular compartments (22, 23, 53). One of the functions of Cav-1 trafficking appears to the maintenance of cholesterol homeostasis (21). Cav-1 binds directly to and is tightly associated with free cholesterol (54), and it travels between the ER and caveolae membrane as a cytosolic complex containing chaperone proteins and cholesterol (55). Another lipid molecule in caveolae tightly associated with Cav-1 is the glycosphingolipid GM1 (56). Thus, Cav-1, together with caveolae (rich in cholesterol and glycosphingolipids), relocates to the cell posterior and provide a second function of caveolin trafficking, *i.e.* establishment of cell membrane polarity in migrating cells. The polarized cholesterol and glycosphingolipids are likely to cause membrane stiffness and reduced deformability at the cell rear (57). Indeed, our previous observation showed the absence of lamellipod protrusions where Cav-1 was polarized (24).

Acknowledgments—We thank Diane Schwegler-Berry for assistance with transmission electron microscopy analysis. BJ5183-AD-1-competent cells and pAdTrack-CMV vector were generous gifts from Dr. Bert Vogelstein of The Johns Hopkins Medical Institutions, Baltimore, MD.

REFERENCES

1. Yamada, E. (1955) *J. Biophys. Biochem. Cytol.* **1,** 445–458
2. Palade, G. E. (1953) *J. Appl. Phys.* **24,** 1424
3. Severs, N. J. (1988) *J. Cell Sci.* **90,** 341–348
4. Parton, R. G., and Richards, A. A. (2003) *Traffic* **4,** 724–738
5. Chini, B., and Parenti, M. (2004) *J. Mol. Endocrinol.* **32,** 325–338
6. Pagano, R. E. (2003) *Philos. Trans. R. Soc. Lond. B Biol. Sci.* **358,** 885–891
7. Pelkmans, L., and Helenius, A. (2002) *Traffic* **3,** 311–320
8. Anderson, R. G., Kamen, B. A., Rothberg, K. G., and Lacey, S. W. (1992) *Science* **255,** 410–411
9. Mineo, C., and Anderson, R. G. (2001) *Histochem. Cell Biol.* **116,** 109–118
10. Mundy, D. I., Machleidt, T., Ying, Y. S., Anderson, R. G., and Bloom, G. S.

(2002) *J. Cell Sci.* **115,** 4327–4339
11. Isshiki, M., Ando, J., Yamamoto, K., Fujita, T., Ying, Y., and Anderson, R. G. (2002) *J. Cell Sci.* **115,** 475–484
12. Engelman, J. A., Zhang, X. L., Galbiati, F., Volonte, D., Sotgia, F., Pestell, R. G., Minetti, C., Scherer, P. E., Okamoto, T., and Lisanti, M. P. (1998) *Am. J. Hum. Genet.* **63,** 1578–1587
13. Scherer, P. E., Lewis, R. Y., Volonte, D., Engelman, J. A., Galbiati, F., Couet, J., Kohtz, D. S., van Donselaar, E., Peters, P., and Lisanti, M. P. (1997) *J. Biol. Chem.* **272,** 29337–29346
14. Way, M., and Parton, R. (1995) *FEBS Lett.* **376,** 108–112
15. Tang, Z.-L., Scherer, P. E., Okamoto, T., Song, K., Chu, C., Kohtz, D. S., Nishimoto, I., Lodish, H. F., and Lisanti, M. P. (1996) *J. Biol. Chem.* **271,** 2255–2261
16. Spisni, E., Tomasi, V., Cestaro, A., and Tosatto, S. C. (2005) *Biochem. Biophys. Res. Commun.* **338,** 1383–1390
17. Anderson, R. G. W. (1998) *Annu. Rev. Biochem.* **67,** 199–225
18. Conrad, P. A., Smart, E. J., Ying, Y. S., Anderson, R. G., and Bloom, G. S. (1995) *J. Cell Biol.* **131,** 1421–1433
19. Scheiffele, P., Verkade, P., Fra, A. M., Virta, H., Simons, K., and Ikonen, E. (1998) *J. Cell Biol.* **140,** 795–806
20. Smart, E., Ying, Y.-S., Conrad, P., and Anderson, R. G. W. (1994) *J. Cell Biol.* **127,** 1185–1197
21. Fielding, C. J., and Fielding, P. E. (1997) *J. Lipid Res.* **38,** 1503–1521
22. Machleidt, T., Li, W. P., Liu, P., and Anderson, R. G. (2000) *J. Cell Biol.* **148,** 17–28
23. Luetterforst, R., Stang, E., Zorzi, N., Carozzi, A., Way, M., and Parton, R. G. (1999) *J. Cell Biol.* **145,** 1443–1459
24. Beardsley, A., Fang, K., Mertz, H., Castranova, V., Friend, S., and Liu, J. (2005) *J. Biol. Chem.* **280,** 3541–3547
25. Parat, M. O., Anand-Apte, B., and Fox, P. L. (2003) *Mol. Biol. Cell* **14,** 3156–3168
26. Ashton, A. W., Yokota, R., John, G., Zhao, S., Suadicani, S. O., Spray, D. C., and Ware, J. A. (1999) *J. Biol. Chem.* **274,** 35562–35570
27. Westermann, M., Steiniger, F., and Richter, W. (2005) *Histochem. Cell Biol.* **123,** 613–620
28. Zicha, D., Dunn, G., and Jones, G. (1997) *Methods Mol. Biol.* **75,** 449–457
29. Song, K. S., Li, S., Okamoto, T., Quilliam, L., Sargiacomo, M., and Lisanti, M. P. (1996) *J. Biol. Chem.* **271,** 9690–9697
30. Ren, X., Ostermeyer, A. G., Ramcharan, L. T., Zeng, Y., Lublin, D. M., and Brown, D. A. (2004) *Mol. Biol. Cell* **15,** 4556–4567
31. Schlegel, A., and Lisanti, M. P. (2000) *J. Biol. Chem.* **275,** 21605–21617
32. Schlegel, A., Schwab, R. B., Scherer, P. E., and Lisanti, M. P. (1999) *J. Biol. Chem.* **274,** 22660–22667
33. Sargiacomo, M., Scherer, P. E., Tang, Z.-L., Kubler, E., Song, K. S., Sanders, M. C., and Lisanti, M. P. (1995) *Proc. Natl. Acad. Sci. U. S. A.* **92,** 9407–9411
34. Scherer, P. E., Tang, Z.-L., Chun, M. C., Sargiacomo, M., Lodish, H. F., and Lisanti, M. P. (1995) *J. Biol. Chem.* **270,** 16395–16401
35. Kurzchalia, T., Dupree, P., Parton, R. G., Kellner, R., Virta, H., Lehnert, M., and Simons, K. (1992) *J. Cell Biol.* **118,** 1003–1014
36. Sargiacomo, M., Sudol, M., Tang, Z.-L., and Lisanti, M. P. (1993) *J. Cell Biol.* **122,** 789–807
37. Liu, J., Oh, P., Horner, T., Rogers, R. A., and Schnitzer, J. E. (1997) *J. Biol. Chem.* **272,** 7211–7222
38. Bickel, P. E., Scherer, P. E., Schnitzer, J. E., Oh, P., Lisanti, M. P., and Lodish, H. F. (1997) *J. Biol. Chem.* **272,** 13793–13802
39. Fra, A. M., Williamson, E., Simons, K., and Parton, R. G. (1995) *Proc. Natl. Acad. Sci. U. S. A.* **92,** 8655–8659
40. Razani, B., Engelman, J. A., Wang, X. B., Schubert, W., Zhang, X. L., Marks, C. B., Macaluso, F., Russell, R. G., Li, M., Pestell, R. G., Di Vizio, D., Hou, H., Jr., Kneitz, B., Lagaud, G., Christ, G. J., Edelmann, W., and Lisanti, M. P. (2001) *J. Biol. Chem.* **276,** 38121–38138
41. Drab, M., Verkade, P., Elger, M., Kasper, M., Lohn, M., Lauterbach, B., Menne, J., Lindschau, C., Mende, F., Luft, F. C., Schedl, A., Haller, H., and Kurzchalia, T. V. (2001) *Science* **293,** 2449–2452
42. Simionescu, M., Gafencu, A., and Antohe, F. (2002) *Microsc. Res. Tech.* **57,** 269–288
43. Schnitzer, J. E., Liu, J., and Oh, P. (1995) *J. Biol. Chem.* **270,** 14399–14404
44. Pelkmans, L., Puntener, D., and Helenius, A. (2002) *Science* **296,** 535–539
45. Hailstones, D., Sleer, L. S., Parton, R. G., and Stanley, K. K. (1998) *J. Lipid Res.* **39,** 369–379
46. Li, S., Couet, J., and Lisanti, M. P. (1996) *J. Biol. Chem.* **271,** 29182–29190
47. Okamoto, T., Schlegel, A., Scherer, P. E., and Lisanti, M. P. (1998) *J. Biol. Chem.* **273,** 5419–5422
48. Venema, V. J., Ju, H., Zou, R., and Venema, R. C. (1997) *J. Biol. Chem.* **272,** 28187–28190
49. Razani, B., Rubin, C. S., and Lisanti, M. P. (1999) *J. Biol. Chem.* **274,** 26353–26360
50. Lee, H., Park, D. S., Razani, B., Russell, R. G., Pestell, R. G., and Lisanti, M. P. (2002) *Am. J. Pathol.* **161,** 1357–1369
51. Li, H., and Papadopoulos, V. (1998) *Endocrinology* **139,** 4991–4997
52. Ostermeyer, A. G., Paci, J. M., Zeng, Y., Lublin, D. M., Munro, S., and Brown, D. A. (2001) *J. Cell Biol.* **152,** 1071–1078
53. Schlegel, A., and Lisanti, M. P. (2001) *Cytokine Growth Factor Rev.* **12,** 41–51
54. Murata, M., Peranen, J., Schreiner, R., Weiland, F., Kurzchalia, T., and Simons, K. (1995) *Proc. Natl. Acad. Sci. U. S. A.* **92,** 10339–10343
55. Uittenbogaard, A., Ying, Y., and Smart, E. J. (1998) *J. Biol. Chem.* **273,** 6525–6532
56. Fra, A. M., Masserini, M., Palestini, P., Sonnino, S., and Simons, K. (1995) *FEBS Lett.* **375,** 11–14
57. Schmidt, C. E., Horwitz, A. F., Lauffenburger, D. A., and Sheetz, M. P. (1993) *J. Cell Biol.* **123,** 977–991

Identification of a Novel Domain at the N Terminus of Caveolin-1 That Controls Rear Polarization of the Protein and Caveolae Formation

Xing-Hui Sun, Daniel C. Flynn, Vincent Castranova, Lyndell L. Millecchia, Andrew R. Beardsley and Jun Liu

J. Biol. Chem. 2007, 282:7232-7241.
doi: 10.1074/jbc.M607396200 originally published online January 8, 2007
